AD-A046 086 WASHINGTON UNIV SEATTLE DEPT OF AERONAUTICS AND AST--ETC F/G 20/4
LIMITS ON LOW SPEED WIND TUNNEL TESTS OF ROTORS.(U)
SEP 77 W H RAE, S SHINDO DA-ARO-D-31-124-72-G019

UNCLASSIFIED ARO-10655.1-E NL

1 OF 1
ADA
046086

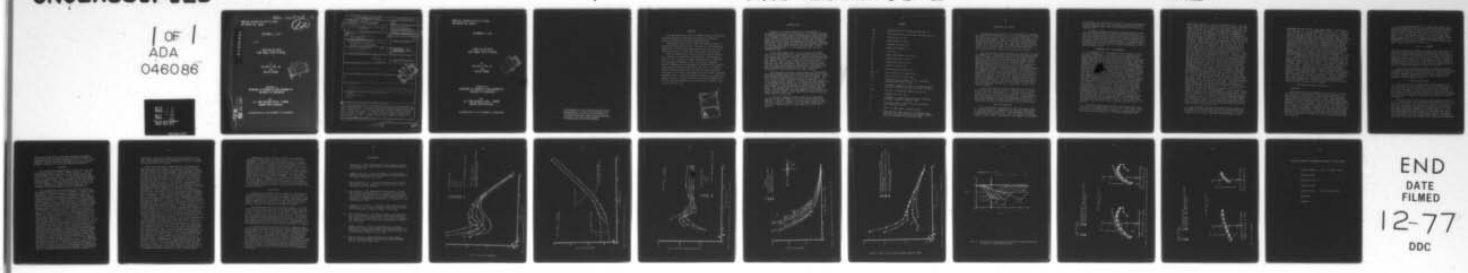

END
DATE
FILMED
12-77
DDC

ARO. 10655.1-E

(12)

GRANT NO. DA-ARO-D-31-124-72-G-0190
ARO PROJECT NO. 10655E

SEPTEMBER 27, 1977

LIMITS ON LOW SPEED WIND TUNNEL TESTS OF ROTORS

BY
WILLIAM H. RAE, JR.
AND
SHOJIRO SHINDO

PREPARED BY
DEPARTMENT OF AERONAUTICS AND ASTRONAUTICS
UNIVERSITY OF WASHINGTON

FOR
U.S. ARMY RESEARCH OFFICE - DURHAM
DURHAM, NORTH CAROLINA

SECURITY CLASSIFICATION OF THIS PAGE (When Data Entered)

REPORT DOCUMENTATION PAGE	READ INSTRUCTIONS BEFORE COMPLETING FORM
1. REPORT NUMBER ARO PROJECT NO. 10655E.1-E	2. GOVT ACCESSION NO.	3. RECIPIENT'S CATALOG NUMBER
4. TITLE (and Subtitle) LIMITS ON LOW SPEED WIND TUNNEL TESTS OF ROTORS,	5. TYPE OF REPORT & PERIOD COVERED Final rept. 5-1-72 to 6-30-77 6. PERFORMING ORG. REPORT NUMBER 1 May 72-30 June 77
7. AUTHOR(s) William H. Rae, Jr. Shojiro Shindo	8. CONTRACT OR GRANT NUMBER(s) DA-ARO-D-31-124-72-G-0190
9. PERFORMING ORGANIZATION NAME AND ADDRESS Department of Aeronautics & Astronautics University of Washington Seattle, Washington 98195	10. PROGRAM ELEMENT, PROJECT, TASK AREA & WORK UNIT NUMBERS
11. CONTROLLING OFFICE NAME AND ADDRESS U. S. Army Research Office Post Office Box 12211 Research Triangle Park, NC 27709	12. REPORT DATE September 27, 1977 13. NUMBER OF PAGES 21
14. MONITORING AGENCY NAME & ADDRESS(if different from Controlling Office) 25 P.	15. SECURITY CLASS. (of this report) Unclassified 15a. DECLASSIFICATION/DOWNGRADING SCHEDULE NA

16. DISTRIBUTION STATEMENT (of this Report)

Approved for public release; distribution unlimited.

DDC RELEASED NOV 1 1977 F.

17. DISTRIBUTION STATEMENT (of the abstract entered in Block 20, if different from Report)

NA

18. SUPPLEMENTARY NOTES

The findings in this report are not to be construed as an official Department of the Army position, unless so designated by other authorized documents.

19. KEY WORDS (Continue on reverse side if necessary and identify by block number)

V/STOL
Wind Tunnel Test
Rotors

20. ABSTRACT (Continue on reverse side if necessary and identify by block number)

The low speed test limit of V/STOL aircraft wind tunnel testing has been investigated and two wall correction theories currently in use have been analyzed. The models used were either rotors or propellers acting as a rotor. In general the test limit based on tail data is more stringent than limits based on rotors. Corrections using Heyson's ε_{eff} are more accurate than traditional wall corrections.

$\varepsilon_{sub\ eff}$

DD FORM 1 JAN 73 1473 EDITION OF 1 NOV 65 IS OBSOLETE

Unclassified

SECURITY CLASSIFICATION OF THIS PAGE (When Data Entered)

370273

GRANT NO. DA-ARO-D-31-124-72-G-0190
ARO PROJECT NO. 10655E

SEPTEMBER 27, 1977

LIMITS ON LOW SPEED WIND TUNNEL TESTS OF ROTORS

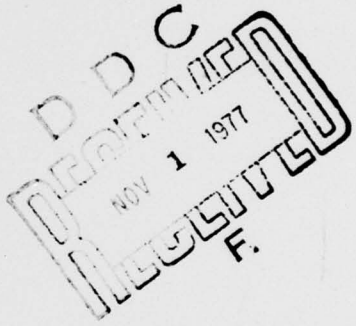

BY
WILLIAM H. RAE, JR.
AND
SHOJIRO SHINDO

PREPARED BY
DEPARTMENT OF AERONAUTICS AND ASTRONAUTICS
UNIVERSITY OF WASHINGTON

FOR
U.S. ARMY RESEARCH OFFICE - DURHAM
DURHAM, NORTH CAROLINA

THE FINDINGS IN THIS REPORT ARE NOT TO BE CONSTRUED AS AN OFFICIAL DEPARTMENT OF THE ARMY POSITION, UNLESS SO DESIGNATED BY OTHER AUTHORIZED DOCUMENTS.

ABSTRACT

The low speed test limit of V/STOL aircraft wind tunnel testing has been investigated and two wall correction theories currently in use have been analyzed.

The models used in this study were either rotors or propellers acting as a rotor. Various size and shape wind tunnel test sections were simulated by the use of inserts installed within a larger main wind tunnel test section.

The low speed test limit has previously been shown to be a function of the model configuration. The extent to which it is a function of model configuration is explored in this paper by adding a tail to the rotor assembly. Several techniques are presented for analyzing the adverse flow condition at the rotor and at the tail. In general, the test limit based on the tail data is more stringent than that at the rotor with respect to the maximum allowable downwash angle. The corrections of Heyson's χ_{eff} technique appear to be more accurate despite the general tendency of all the methods towards over correction of the data, relative to the free air.

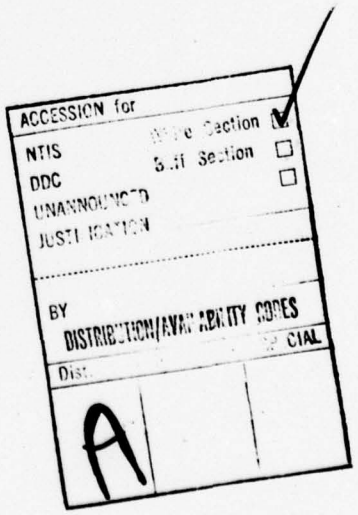

INTRODUCTION

Testing of a V/STOL vehicle in a wind tunnel is accompanied by several problems which are directly related to the large downwash angles associated with these vehicles. The fundamental requirements in developing corrections are: first, to deal with the constraint of the flow around the model due to the tunnel boundaries and second, to treat a wake which may be deflected substantially downward from the horizontal. This paper presents the comparison and results of the applicability of Glauert's theory (Ref. 1) and Heyson's method (Ref. 2) to a series of rotor and tail aerodynamic data.

It has been shown (Ref. 3) that testing of V/STOL vehicles in wind tunnels in transition speed ranges leads to a flow condition which causes a severe distortion of the flow around the model. Thus, the resulting flow field does not resemble that of free flight out of ground effect. When the low speed testing reaches this condition, it is believed that the aerodynamic data are no longer correctable by either techniques referenced above, and great care must be exercised to interpret the data. This adverse phenomenon has been referred to as flow breakdown.

Over the past few years, the University of Washington has been experimentally investigating the behavior of V/STOL wind tunnel models operating in the transition range. This work has been accomplished by the use of two models: one, a 3.14 foot diameter hinged rotor and the second, a 2.02 foot diameter rigid propeller. Various sizes and geometries of open-ended boxes constructed of plywood and plexiglass were inserted in the University of Washington 8 x 12 foot wind tunnel to simulate different size and shape test sections. The method used here eliminated the undesirable effect of both Reynolds and Mach numbers while studying the tunnel boundary effect on the model with various ratios of model size to tunnel size.

It has been generally agreed that wall corrections applied at the tail tend to be less accurate than those applied to angle of attack, lift and drag at the main lifting body. For this reason, a tail has been added to the 2.02 foot diameter rotor to study the flow in the tail region.

SYMBOLS

A_m	Momentum area of lifting system; sq. ft.
A_T	Cross-sectional area of test section; sq. ft.
C_L	Coefficient of lift
C_D	Coefficient of drag
D	Diameter or rotor; ft.
H	Height of tunnel; ft.
L	Lift; lbs.
q	Dynamic pressure; lbs./sq.ft.
S	Rotor disk area; sq. ft.
$v\alpha$	Freestream velocity; fps
W	Width of tunnel; ft.
x	Longitudinal location; ft.
$\alpha NF = 0$	Zero normal force angle; deg.
αR	Rotor angle of attack; deg.
Δi_t	Boundary-induced change in tail incidence, positive with nose up; deg.
$\Delta\alpha$	Equivalent change in angle of attack caused by boundary interference, positive nose up; deg.
$\delta W,L$	Vertical interference factor due to lift
ε	Downwash at tail; deg.
θ_n	Deflection of wake from horizontal, measured at model, positive downward; deg.
μ	Tip speed ratio, freestream velocity/blade tip rotational speed
σ	Ratio of model span to tunnel width
χ	Momentum wake skew angle, angle between wake and vertical axis of tunnel, measured at model, positive rearward from vertical; deg.

APPARATUS AND TESTS

All tests were conducted in the University of Washington Aeronautical Laboratory 8 x 12 ft. low speed wind tunnel. The test section size and width to height ratio were varied by the use of plywood inserts, according to the method described in Reference 4. The two important parameters that are involved in this study are: one, the tunnel width to height ratio (W/H) and two, the model span to tunnel width ration (σ). Six test section configurations were used during this program. They are: 8 x 12 ft. (H x W), 3 x 6 ft., 4 x 6 ft., 3 x 4.5 ft., 6 x 4 ft., and 4 x 4 ft.

The tunnel's main balance system was used and is capable of measuring six components individually and simultaneously. The lift, drag, and pitching moment of the rotor which was mounted on the balance were measured with respect to the wind axis and were read visually from the balance meters. Rotor angle of attack was varied remotely from -7 to +7 degrees, measured relative to the test section centerline. The rotor rpm was held constant for all test conditions. The model was placed at the center of the testsection during this series of tests. A tail was added to the rigid 2.02 ft. diameter rotor at one rotor diameter aft of the hub. A mechanical linkage system maintained this tail relative position in the rotor tip path plane when the rotor angle of attack was changed. The tail was mounted on the top of a tail strut which housed a pair of strain gauges to measure the tail normal force. The entire assembly was mounted on the non-metric main balance fairing. Thus the tail normal force was measured mechanically independent of the rotor balance reading.

A series of nominal rotor tip speed ratios from 0.20 to 0.05 was used for all testing. The flow in the region of the tail was investigated at a constant rotor angle of attack (-3°) in conjunction with a series of tail angles of attack applied at each tip speed ratio. These test data were then corrected to free air conditions by available correction methods and then tests were run in the 8 x 12 ft. test section using the corrected data as test conditions.

FLOW CALIBRATIONS

The inserts were constructed so that the walls could be tapered outward to compensate for boundary layer growth in the longitudinal direction. Measured static pressure longitudinal distribution was used to determine the proper amount of wall taper. The test section upflow in the region

of the rotor was calibrated by using a 6 inch chord symmetrical calibration wing. The upflow was measured at several values of dynamic pressures corresponding to the test tip speed ratios.

A dynamic pressure calibration was necessary to correlate the indicated dynamic pressures obtained from the q - balance with the actual dynamic pressure in the rotor region. This was accomplished by surveying the dynamic pressure in the rotor region and then taking the average value as representative of the actual dynamic pressure. Care was taken to measure the insert indicated dynamic pressures far enough upstream from the rotor so as to avoid any effects of the rotor pressure field.

PHENOMENA OF FLOW BREAKDOWN

The mechanics of flow breakdown are outlined in some detail in Reference 3. Basically, flow breakdown occurs when the interaction of the wake with the test section boundaries and with the main tunnel flow induces a blockage effect which distorts and invalidates test data. This adverse condition can be characterized by two concurrent flow phenomena. The first is the motion of the downwash wake forward along the floor of the test section as the downwash angle increases and the second is the motion of the wake laterally across the floor spreading in a horseshoe pattern and then, under certain conditions, the wake moves up along the test section walls. For convenience, these are termed the floor effect and the secondary effect, respectively. The complex nature of these flow conditions inhibits analytical studies and avails itself more readily to an empirical analysis. Reference 3 contains the results of experiments in rectangular test sections with width to height ratios, W/H, from 0.5 to 1.5 and model area to test section area ratios, A_m/A_t, as high as 0.6. The conclusions reported in Reference 3 were based upon the effects of flow breakdown on the rotor aerodynamic characteristics. The flow breakdown point, which often is not clearly definable, is parameterized as a maximum momentum downwash angle, Θ_n. The present study used a tail to study the flow in the region one diameter aft of the rotor hub. The methods used to identify the flow breakdown effect in this region are described and the resulting test limits for the tail region are then compared to the limits obtained for the rotor itself.

Since the amount of deviation in the insert data from those of 8 x 12 (equivalent to free air) is the main criterion used to establish their validity, it is desirable that the test data be studied in a form which emphasizes the

deviations occuring at the flow breakdown point. For the tail region this can readily be seen by plotting the downwash at the tail (ε) versus the tip speed ratio (Fig. 1). Figure 1 shows that as the tip speed ratio decreases from 0.20, which is equivalent to increasing the momentum downwash angle, the downwash at the tail increases until some values of tip speed ratio at which the downwash at the tail begins to decrease. The initial formation of the parabolic shaped vortex-like flow on the floor takes place at the tip speed ratio when the downwash at the tail is at its peak. Upon formation, the apex of this flow on the floor is well aft of the model. The rotation of this vortex-like flow is clockwise viewed from the left side with tunnel flow from left to right, and deflects the rotor wake upwards, thereby causing an upwash which has the net effect of reducing the downwash at the tail. As the tip speed ratio continues to decrease, there is a sudden increase in the downwash at the tail. At this point the flow in the vicinity of the tail is severely distorted, and the condition is defined as the flow breakdown point. As the apex of the parabolic flow on the floor moves upstream of the tail, the vortex-like flow causes an additional downwash at the tail, thus increasing the total downwash. This leads to an inflection point in the curve corresponding to the point at which the vortex-like flow on the tunnel floor affects the test results. When the secondary effect is minimized, the inflection is gradual and the flow breakdown occurs over a region rather than at a point. Such is the case for the 3 x 6, 4 x 6, and 3 x 4.5 inserts which have width to height ratios greater than one. Note that the 8 x 12 test section provides the equivalent free air case where the wall effects are minimal and there is no inflection in the curve. A study of this figure shows that the maximum allowable downwash angle which corresponds to the minimum allowable tip speed ratio increases in the following order: 4 x 6, 3 x 6, 3 x 4.5 inserts. The greater downwash allowed in the 4 x 6 as compared to the 3 x 6 is attributable to the stronger floor effect in the latter. The stronger secondary effect in the 3 x 4.5 causes its allowable momentum downwash to be less than that of the 3 x 6 insert. A larger momentum downwash is allowed in the 6 x 4 since the floor effect is reduced in comparison to the 4 x 4. As the model to tunnel size ratio increases, the allowable momentum downwash decreases. Thus, the determining factor in the importance of the secondary effect is the ratio, D/W.

Over the past few years, the major effort devoted to the study of flow breakdown has been directed toward the analysis of the flow in the region of the rotor. Figure 2 illustrates the typical approach used to identify flow

breakdown in this region. The rotor angle of attack was held constant at -3° (corresponding to drag = 0). The rotor lift for the 4 x 6 insert and the 8 x 12 tunnel is plotted versus rotor tip speed ratio. The expected curve is based upon the assumption that the rotor is operated free of any floor or secondary effects described earlier. The difference in lift between the free air and wind tunnel increases as the lift coefficient increases or equivalently as the rotor tip speed ratio decreases for a constant angle of attack operation. Note that the curve representing the smaller test section is close to the 8 x 12 curve at high tip speed ratios (low C_L's), and at low tip speed ratios the curves diverge. The point at which the data diverge from the expected curve is identified as the flow breakdown point. Another technique to identify the adverse condition is to use the lift curve slope rather than the lift, as shown in Figure 3. Comparison of lift curve slopes between the equivalent free air (8 x 12) data and inserts data shows that, at some low values of tip speed ratio, the curves diverge; for example, at 0.073 for 4 x 6 insert. The abnormal behavior of these insert curves at low tip speed ratio, relative to the free air, is similar to that of the curves shown in Figs. 1 and 2. The tip speed ratio at which the insert curves diverge from the free air data is again used to define the flow breakdown point. The functional relationships between Θ_n and the area ratio, A_m/A_t for varying values of W/H, represent the limiting conditions. Figure 4 presents test limit curves for a variety of test section configurations, as determined by the methods outlined previously. This figure shows that even more severe limitations are encountered when there is a tail present.

APPLICATION OF WALL CORRECTIONS

THEORIES

The conventional representation of the wake, which does not account for the wake vertical deflection, seems to be significantly inadequate for V/STOL models where the wake may be deflected by as much as 90°. Thus, the fundamental requirement in developing corrections for V/STOL wind tunnel tests is to treat a wake which may be deflected substantially downward from the horizontal. Since Glauert's theory does not account for the deflected wakes and has the assumption of small correction angles, it does not correct the tunnel velocity. Hence, this theory corrects only the angle of attack and the drag at the rotor. At the tail, the correction was applied to the angle of attack because only the tail normal force was required to correct the tail pitching moment about the rotor hub.

In a more advanced theory of V/STOL wind tunnel wall correction methods, Heyson considers the wake of any generalized lifting system to be represented by a semi-infinite string of point doublets whose axes are tilted by some angle related to the lift and drag of the lifting system (Ref. 2). In the present study, the effective wake skew angle, χ_{eff}, was used in the application of Heyson's theory. As defined in Ref. 2, the momentum wake skew angle, χ is measured from the vertical plane. The effective wake skew angle χ_{eff}, is defined by: (Ref. 5)

$$\chi_{eff} = \frac{\chi + 90°}{2}$$

The wake of Heyson's mathematical model leaves the model at an effective skew angle and moves downward at this angle until it intersects the tunnel floor and then it trails aft along the floor. The performance of the model in the wind tunnel is equivalent to the performance in free air with an increased rate of sink and an increased velocity. These increases lead to corrections in the angle of attack, drag, and dynamic pressure at the rotor; and to corrections in the angle of attack and dynamic pressure at the tail.

The major difference between the theories of Glauert and Heyson is that the latter computes the horizontal induced velocity and corrects the tunnel velocity. This results in a dynamic pressure correction which, when applied to the rotor at constant nominal tip speed ratios, results in a change in the tip speed ratios.

TESTING PROCEDURES

The rotor and tail assembly was first tested in the inserts, with the rotor pitched to an angle of attack of -3°. The ratio of the freestream velocity of the tunnel to the rotor tip speed, μ, was varied from 0.20 to 0.05 by decreasing the tunnel dynamic pressure. After each run the tail angle of attack was changed and the process was repeated. The tail angle of attack was changed from 10° to 25° in 5° increments.

The rotor and tail assembly was then tested in the 8 x 12 ft. test section. The test program in the 8 x 12 ft. test section was divided into two parts: During the first part, the test conditions, tip speed ratio and angle of attack were kept the same as those in the inserts to allow for direct data comparison between the tunnels (Figs. 1, 2 & 3). This comparison was used primarily to determine the point of flow breakdown for the rotor and the tail. The insert data were then corrected to equivalent free air conditions using both Glauert's and Heyson's wall correction techniques.

During the second part of the test program, the insert corrected values of dynamic pressure and rotor angle of attack were used as test conditions in the 8 x 12 ft. test section. The tail was again pitched to each of its four angles of attack for each rotor operating condition.

ANALYSIS

The uncorrected downwash angle at the tail at a constant rotor angle of attack is shown in Fig. 1. While a characteristic dip is present in all insert data in the low tip speed ratio range, it is not discernible in the 8 x 12 ft. test section data. As explained in the earlier section, this behavior is attributable to the flow breakdown phenomena. Since the walls and floor of the 8 x 12 ft. test section are located furthest away from the rotor and tail assembly in comparison to the inserts, the influence of flow breakdown is almost nonexistent.

The uncorrected data were then corrected using the correction theories of Glauert and Heyson. Figure 5 shows the effect of the corrections as applied to the 4 x 4 ft. insert data. There is a good correlation between the Glauert correction and Heyson correction at tip speed ratios higher than 0.10, although they tend to over correct relative to free air. At lower values of tip speed ratio, the flow begins to break down and the correlation is poor. Note that Glauert's standard theory adds a larger increment to the uncorrected data. The good agreement between the theories even at relatively large values of $\Delta\alpha$ is due to the behavior of Heyson's vertical interference factors, $\delta_{W,L}$. At high lift coefficients, (low χ_{eff}) these factors tend to be significantly greater in magnitude than the equivalent factors of Glauert's theory. However, for values of χ_{eff} greater than 75° to 80°, the magnitude of $\delta_{W,L}$ remains about constant at a value equivalent to that of conventional theory (Refs. 2 and 6). As noted above, at the more extreme conditions where the indicated average correction angles are very large, Heyson's corrections are significantly less than those of the conventional theory. In addition to this, Heyson's theory also adds a horizontal interference which tends to increase the correction angle. The small angle assumption in conventional theory tends to increase the size of the indicated correction angle substantially over that which would be obtained without this assumption. Under certain testing conditions, a singularity may occur such as shown in Fig. 5 at $\mu = 0.07$ between the data of the 4 x 4 uncorrected and the 8 x 12 corrected, equivalent to free air. The angle of zero normal force at the tail in the 8 x 12 at this tip speed ratio appears to coincide with that of the 4 x 4 uncorrected data which may lead to a conclusion that the data obtained in the smaller test section under this particular testing condition are

equivalent to free air without any wall correction. However, such conclusions are erroneous because as it can be seen in the same figure, the corrected 4 x 4 data no longer coincide with the 8 x 12 data.

Note also in Figure 5 that there is a divergence between the corrected insert curve and the free air curve. The beginning of divergence corresponds to the point where the tail encounters flow breakdown. The divergence is also enhanced in the low μ range by the break down of the flow in the region of the rotor. Note that for the inserts, a decrease in the tip speed ratio corresponds to an increase in the zero normal force angle at the tail. This is not the case for the 8 x 12 ft. test section. At a tip speed ratio of 0.085, the angle of zero normal force begins to decrease and continues to do so until a tip speed ratio of 0.056 is reached, at which point it again begins to increase. The reason for this behavior is suggested by Heyson in Reference 8. The corrections at the tail are larger than those at the rotor when the lift coefficients are moderate; but, at the more extreme lift coefficients, there is gradually a tendency for the interference at the rotor to exceed that at the tail. Examination of the longitudinal distribution of interference factors in Ref. 2 indicates the reason for this behavior. As shown in Fig. 6, the peak vertical interference for $\chi = 0°$ occurs at the model, and as χ increases the location of the peak interference shifts to even greater distances behind the model. In his discussion, Heyson defines Δi_t as the difference between the interference at the location of the tail and the interference at the location of the rotor. Δi_t will be positive if the momentum wake skew angle is large enough to place the maximum interference behind the tail. Δi_t will decrease once the point of maximum interference moves forward in front of the tail. Further forward movement of the point of maximum interference will eventually, at some small wake skew angle, lead to a condition where the interference at the tail is less than that at the rotor and Δi_t will become negative. Note that this change in sign of Δi_t occurs for conditions above the flow breakdown limit at the tail, but below the flow breakdown limit at the rotor. Δi_t again becomes positive once the flow breakdown limit at the rotor has been exceeded. In the inserts, the interference at the tail is always greater than that at the rotor. Hence Δi_t is always positive and the characteristic dip recorded in the μ range of 0.07 to 0.08 is absent. However, Δi_t does decrease as the flow breakdown limit is approached. This accounts for the flattening of the curves in the tip speed ratio range of 0.08 to 0.12. Below $\mu = 0.08$ the extreme increase in the tail efficiency causes Δi_t to increase rapidly. This results in the largest increment in the zero normal force angle for a corresponding constant decrease in the tip speed ratio.

Additional series of pitch runs were also made by varying the rotor angle of attack from -7° to +7° in 2° increments. These data are corrected to free air using Glauert's and Heyson's wall correction methods. Figure 7 shows the results of applying these corrections to 3 x 4.5 insert rotor data. Heyson's method applied to the data at the tip speed ratio of 0.06 (θ_n = 48°) shown in Fig. 7-a results in closer agreement with the free air than Glauert's method both in lift and drag coefficients. At the low tip speed ratio, Heyson's method can correct the lift curve slope better than the classical method. At a higher tip speed ratio, for example, at 0.125, both corrections result in a near perfect agreement as shown in Fig. 7-b. The pitching moment correction can be examined by studying Fig. 5 which shows that the induced flow in the tail region can be corrected by Heyson's method closer to free air than with Glauert's method.

CONCLUSIONS

There is, when testing V/STOL models in a wind tunnel, a minimum speed test limit that is caused by an adverse change in the flow field around the model. This flow field change is caused by an interaction between the model's high energy wake, the main tunnel flow, and usually the tunnel floor. The point at which this occurs is a function of several factors including the model configuration.

Several methods have been presented whereby it is possible to identify the onset of this adverse flow. The flow in the region of the rotor can be analyzed by examining the change in either the rotor lift curve slope or the rotor tail can be analyzed by studying the variation in the angle of zero normal force with the tip speed ratio. Previously, test limits have been established by analyzing the flow in the region of the primary source of lift. The present study has demonstrated that even more severe limitations are encountered when the flow in the region of the tail is studied.

It has been shown that Glauert's wall correction techniques may be used for rotors as long as the downwash angles do not exceed 23° (which included tip speed ratios from 0.20 through 0.125 for the rotors tested). For downwash angles greater than 23° it is shown that Heyson's χ_{eff} theory provides better wall corrections than Glauert's theory does. For downwash angles from 32° to 58° (which corresponded to tip speed ratios from 0.09 through 0.05 for the rotors tested) the classical wall corrections did not correctly account for the lift curve slope change while Heyson's corrections did account for this. Care must be taken to compare the data at constant tip speed ratios in order to obtain a correct data comparison.

REFERENCES

1. Glauert, H., "The Interference on the Characteristics of an Airfoil in a Wind Tunnel of Rectangular Section", R & M 1459, 1932.

2. Heyson, Harry H., "Linearized Theory of Wind-Tunnel Jet Boundary Corrections and Ground Effect for VTOL-STOL Aircraft", NASA TR R-124, 1962.

3. Rae, William H., Jr., "Limits on Minimum-Speed V/STOL Wind Tunnel Tests", Journal of Aircraft, Vol. 4, No. 3, May-June, 1967, pp. 249-254.

4. Lee, Jerry L., "An Experimental Investigation of the Use of Test Section Inserts as a Device to Verify Theoretical Wall Corrections for a Lifting Rotor Centered in a Closed Rectangular Test Section", Master's Thesis, University of Washington, Department of Aeronautics and Astronautics, 1964.

5. Heyson, H. H. and K. J. Grunwald, "Wind Tunnel Boundary Interference for V/STOL Testing", Conference on V/STOL and STOL Aircraft, Paper 24, NASA SP-116, 1966.

6. Rae, William H., Jr. and Shojiro Shindo, "An Experimental Investigation of Wind Tunnel Wall Corrections and Test Limits for V/STOL Vehicles", University of Washington, Department of Aeronautics and Astronautics, Report No. 73-1, 1973.

7. Heyson, Harry H., "Use of Superposition in Digital Computers to Obtain Wind-Tunnel Interference Factors for Arbitrary Configurations, With Particular Reference to V/STOL Models", NASA TR R-302, 1969.

8. Heyson, Harry H., "Rapid Estimation of Wind-Tunnel Corrections with Application to Wind-Tunnel and Model Design", NASA TN D-6416, 1971.

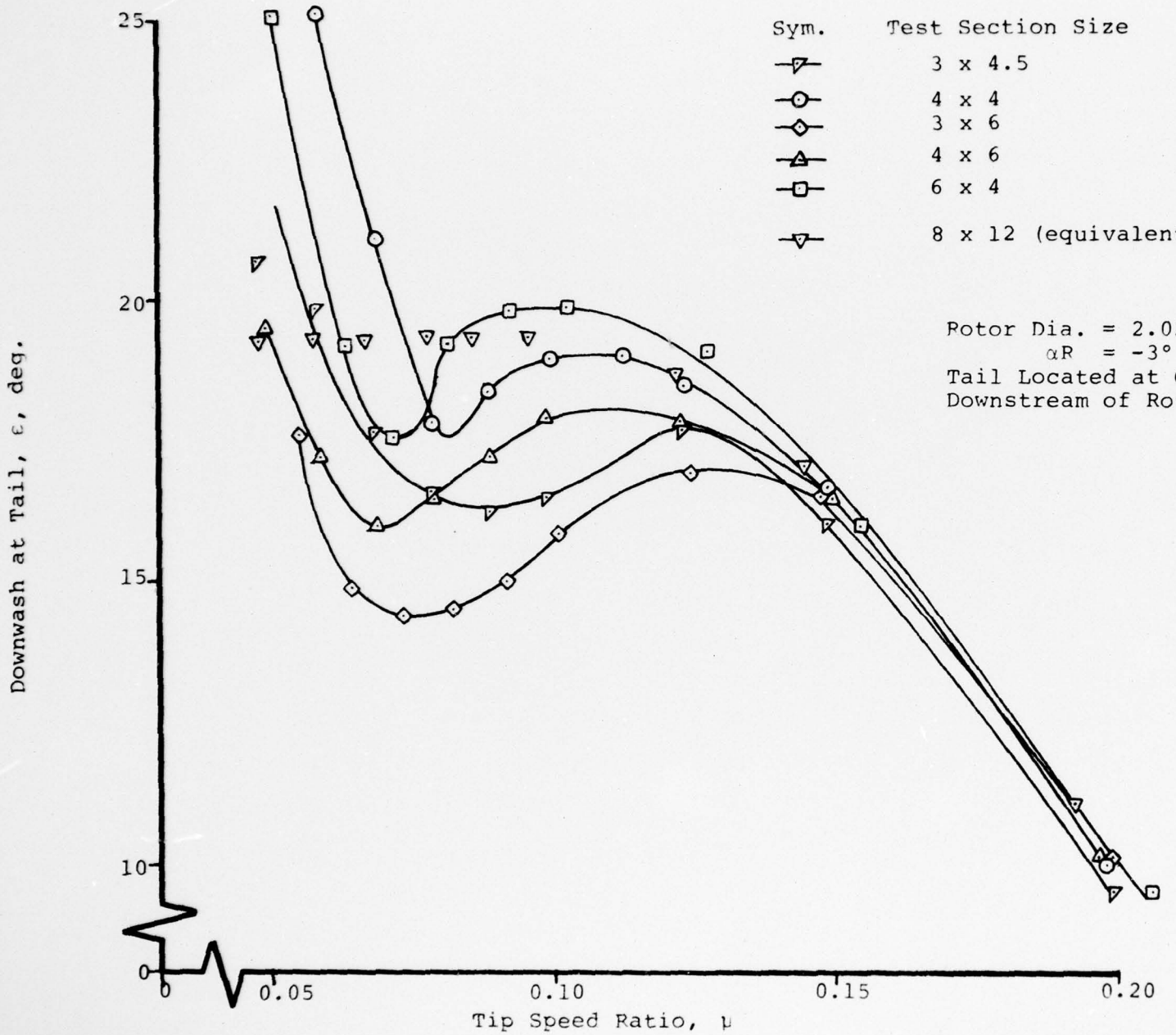

FIG. 1. Uncorrected Downwash Angle at Tail.

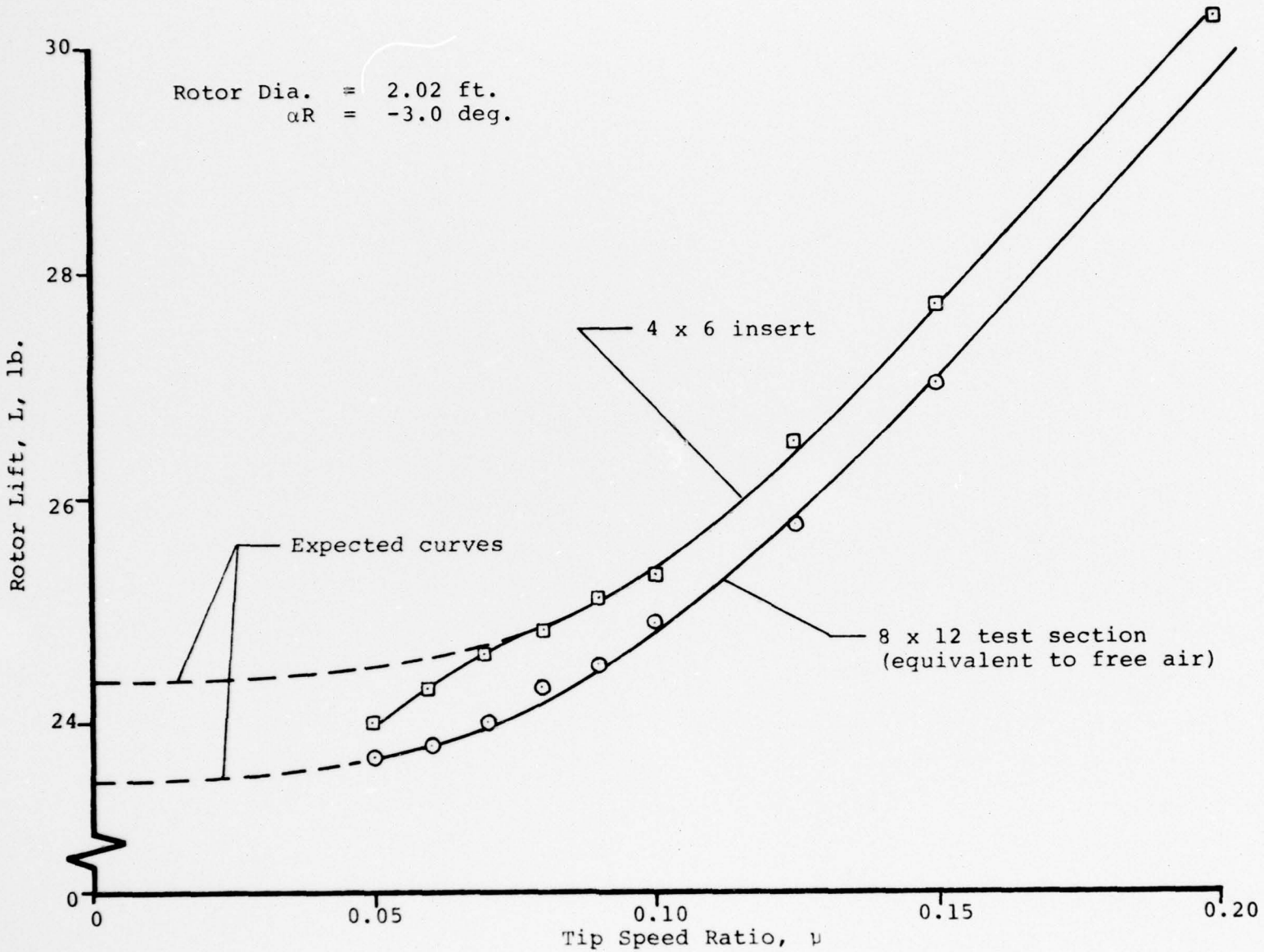

FIG. 2. Effect of Flow Breakdown on Rotor Lift

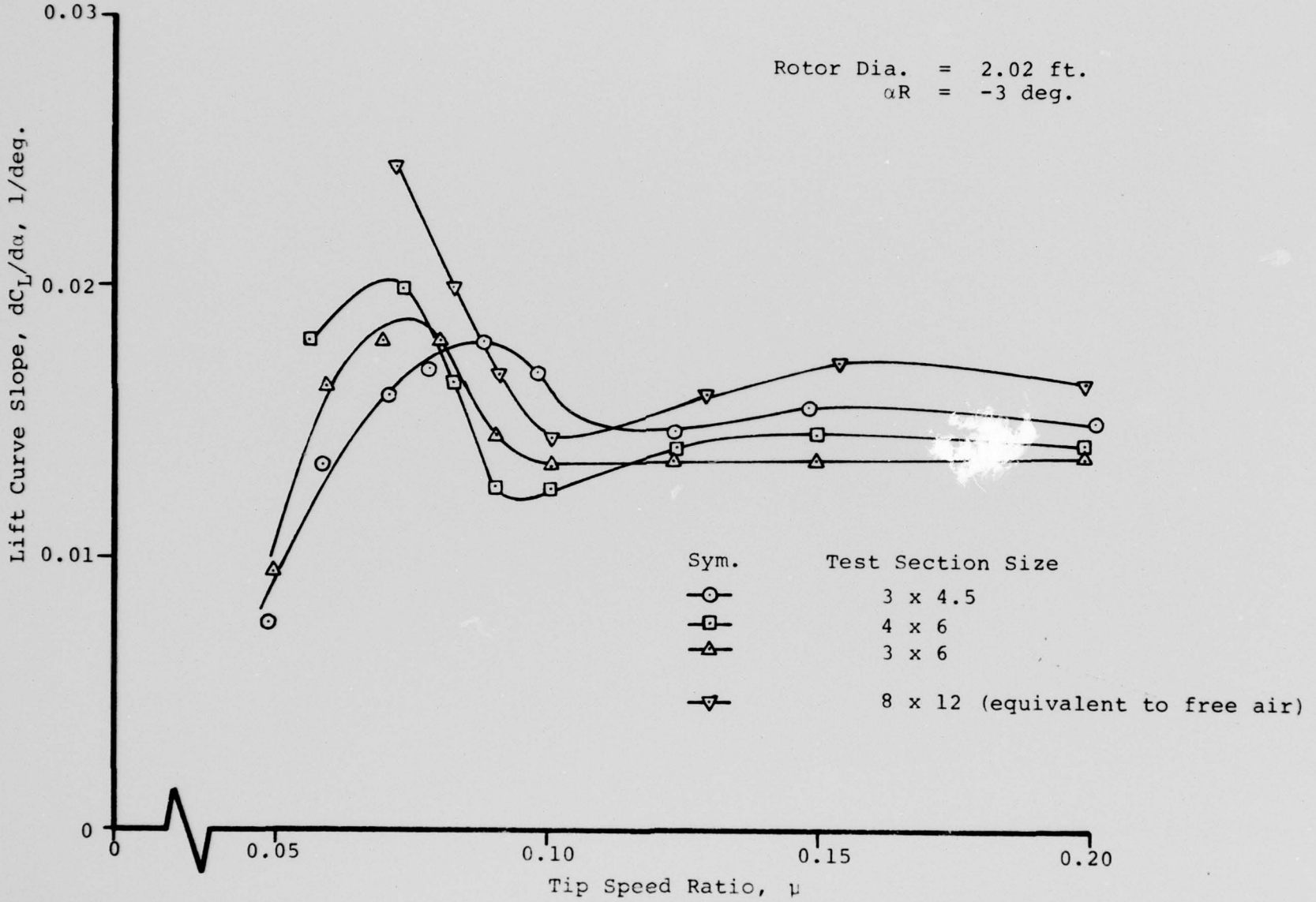

FIG. 3. Effect of Flow Breakdown on Rotor Lift and Curve Slope.

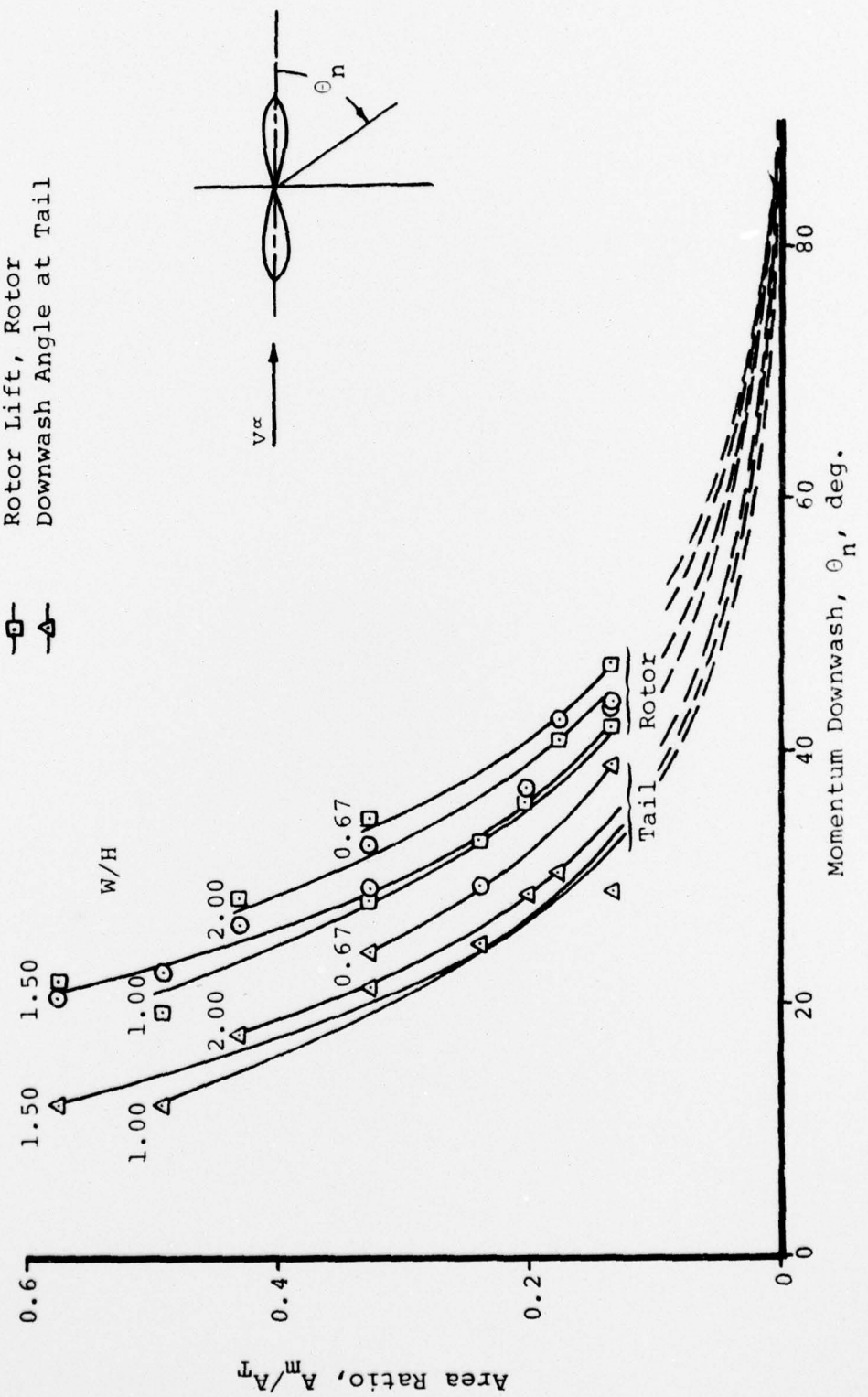

FIG. 4. Test Limites Due to Flow Breakdown for Rotor and Tail

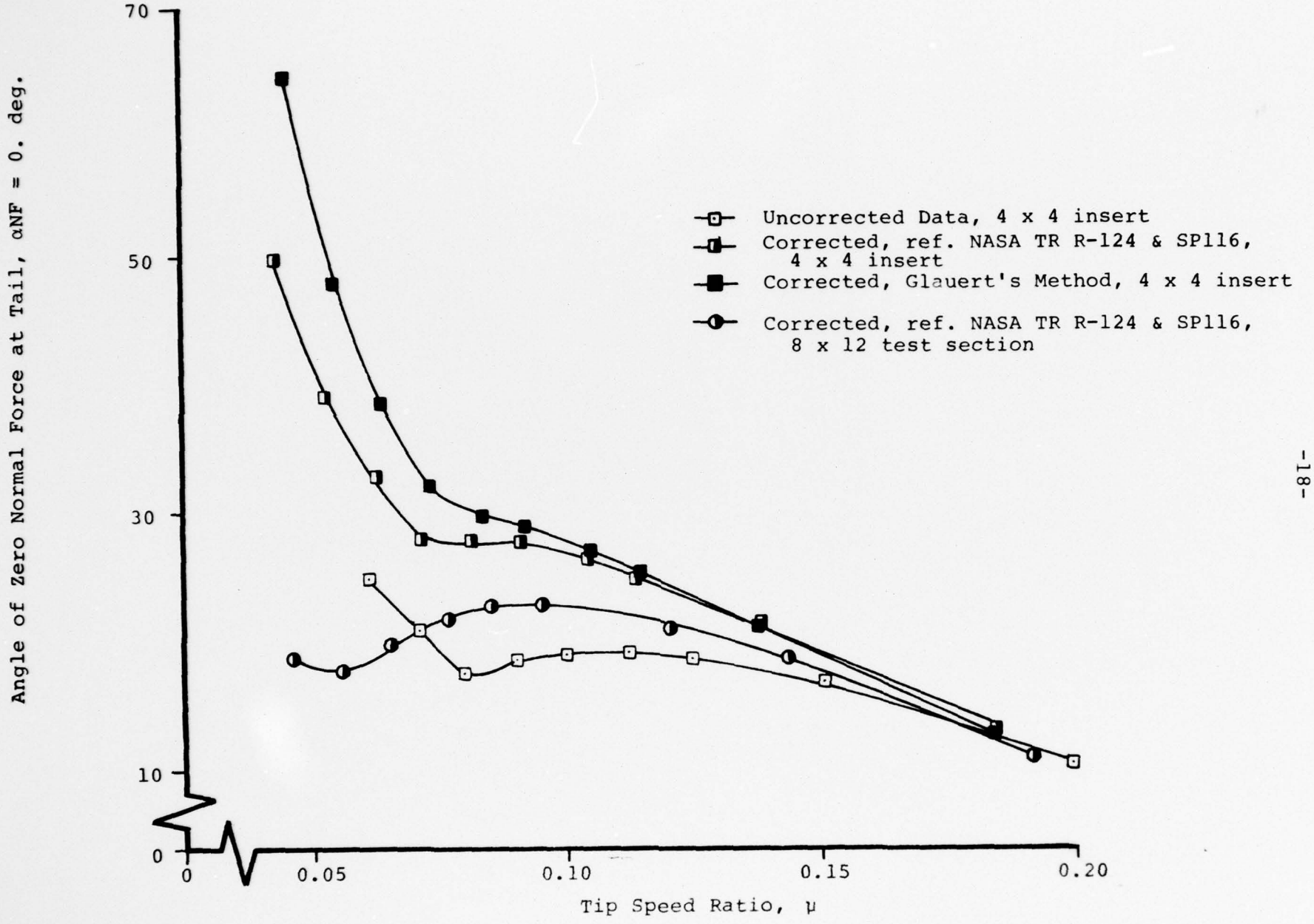

FIG. 5. Comparison of Correction Methods Applied to Downwash at Tail.

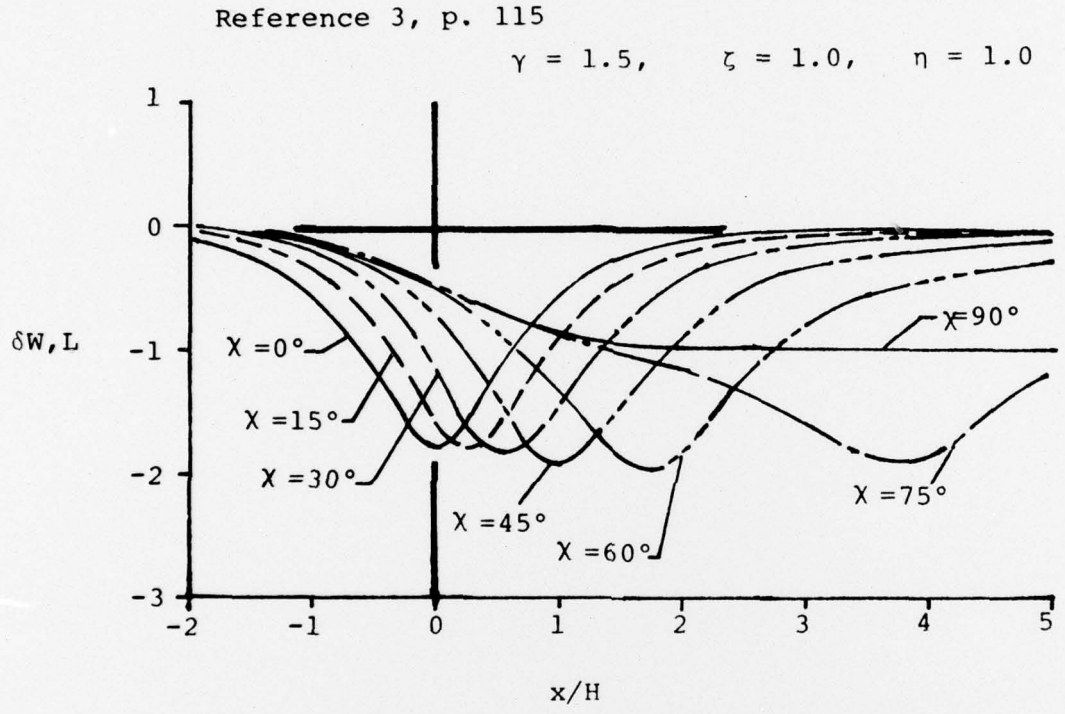

FIG. 6. Longitudinal Distribution of Vertical Interference Due to Lift in a Closed Wind Tunnel.

Test Section
8x12 3x4.5

- Uncorrected Data
- Corrected, ref. NASA TR R-124 & SP116
- Corrected, Glauert's method

Rotor Dia. = 2.02 Ft.
μ = 0.06

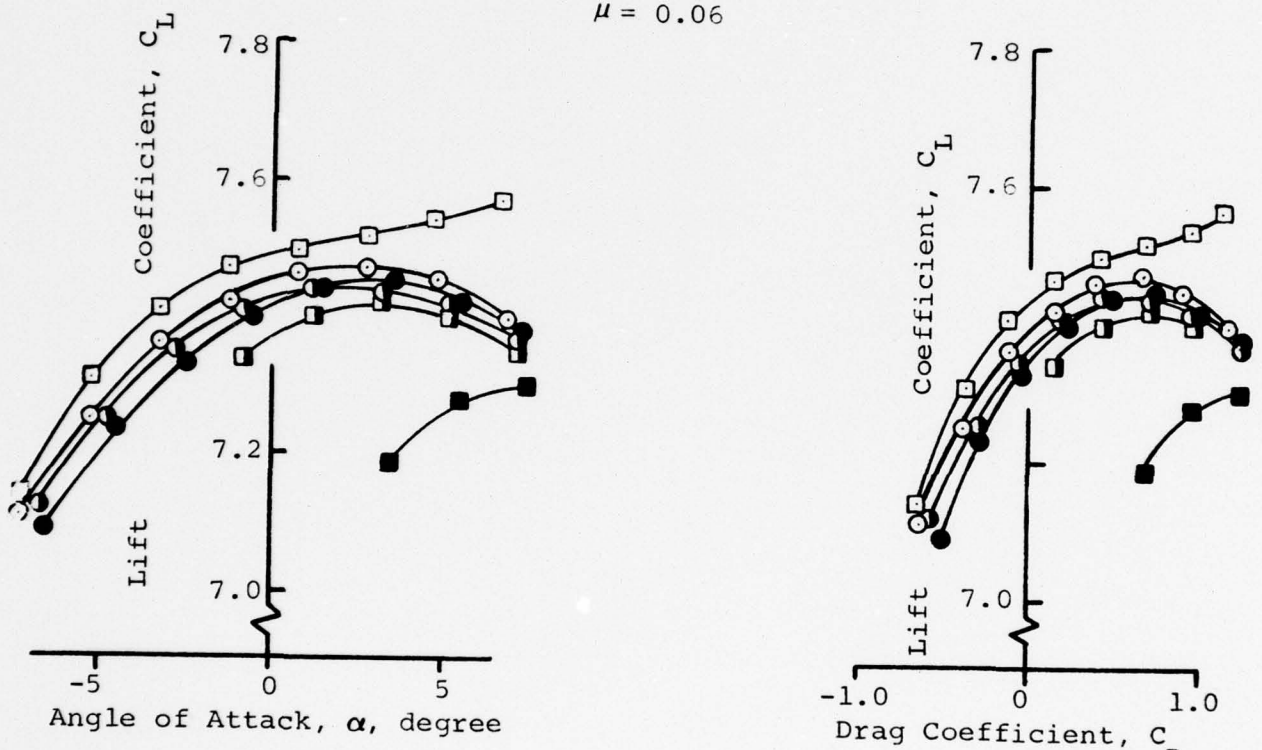

FIG. 7-a. Rotor Lift and Drag, With and Without Jet Boundary Correction.

Test Section
8x12 3x4.5

- Uncorrected Data
- Corrected, ref. NASA TR R-124 & SP116
- Corrected, Glauert's method

Rotor Dia. = 2.02 Ft.
μ = 0.125

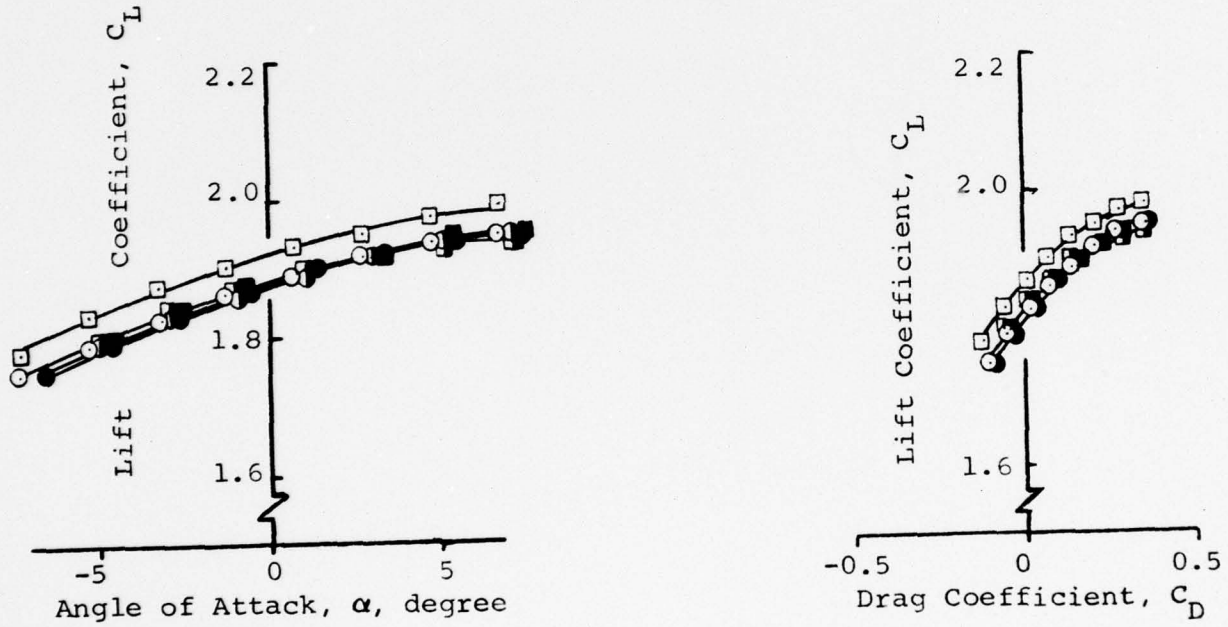

FIG. 7-b. Concluded.

LIST OF SCIENTIFIC PERSONNEL SUPPORTED BY THIS GRANT

Shinjiro Miyata - M.S. in March, 1974

Tsuneo Noguchi

William H. Rae, Jr.

Shojiro Shindo

Calvin Titera - M.S. in March, 1974

David Wei

James Wu